ANALYSIS OF STRUCTURAL DEFORMATION-INDUCED SUN TRACKING ERROR IN A 5-KW HIGH CONCENTRATOR PHOTOVOLTAIC SYSTEM

Chih-Kuang Lin[1], Yan-You Liu[1], Jiunn-Chi Wu[1], and Hwa-Yuh Shin[2]

[1] Department of Mechanical Engineering, National Central University, Jhong-Li 32001, Taiwan

[2] HCPV System R&D Project, Institute of Nuclear Energy Research, Lung-Tan 32546, Taiwan

Abstract

The purpose of this study is using finite element analysis (FEA) to investigate the effects of gravity and wind loads on the structural deformation and concentrator misalignment in a 5-kW high concentrator photovoltaic (HCPV) system. Several operation conditions, including no wind and wind speeds of 7 and 12 m/s blowing to the front side and back side of concentrator arrays, were applied to simulate the stress distribution and structural deformation in the given solar tracker. The concentrator misalignment caused by the structural deformation was also calculated. A comparison of the simulation and measurement results of strain change at two selected locations in the given solar tracker during field operation was made to validate the constructed FEA model. A reasonable agreement of the simulation and measurement results was found such that the constructed FEA model was validated to be effective in assessment of the structural integrity of an HCPV system. No structural failure was predicted for all the components in the given solar tracker under the loading conditions of gravity alone and plus a wind speed of 7 or 12 m/s according to the von Mises failure criterion. An agreement in the trend of variation of misalignment and resultant displacement of Fresnel lens in each concentrator was found. Therefore, the concentrator with a greater misalignment could be readily identified from the corresponding displacement distribution. Given the conditions of no wind and wind speeds of 7 and 12 m/s, the maximum concentrator misalignment was of 0.3^o for a wind speed of 12 m/s blowing to the front side of concentrator arrays and it was within the range of an acceptance angle of 0.4^o for the given concentrator.

1. Introduction

A high concentrator photovoltaic (HCPV) system is usually incorporated with a solar tracker to maintain a very high efficiency of concentrator solar cells (Luque et al., 2006; Luque and Andreev, 2007; Willeke, 2003). Concentrator modules are mounted on a tracking mechanism which keeps the lens and cell directed toward the sun. To ensure that the sunlight can be correctly focused on the concentrator solar cells in an HCPV system, it needs to precisely control the position of the concentrator modules corresponding to the sun. For an HCPV system, the solar tracking accuracy is a critical issue. If the efficiency of a concentrator module drops to 90% of the maximum power for an incident angle, this incident angle is defined as acceptance angle. In order to maintain a very high efficiency in HCPV systems, the required tracking error should be less than their own acceptance angle during operation. Structural deformation is one of the tracking error sources in an HCPV system. It is mainly due to the weight of concentrator modules and the wind loads acting on the concentrator modules. An HCPV solar tracker is always attached with numerous concentrator modules which have heavy weight and a large area subjected to wind loads. Therefore, assessment of the structural deformation in the solar tracking assembly and the induced solar tracking misalignment is necessary for design of a precise and reliable HCPV system.

An HCPV system with a solar tracker of pedestal form is particularly sensitive to wind loads, since the drive mechanism must support both self-weight and wind loads (Luque and Hegedus, 2003). For reliable operation of a solar tracker, it is required that its structure should be able to withstand its own weight and external wind loads, and to keep its deformation below a certain threshold such that the acceptance angle loss of its concentrator modules remains within certain tolerable bounds. Therefore, structural stress and deformation analysis is necessary for a successful, effective design of a precise solar tracker and installation of a reliable HCPV system with required performance,. However, only a few studies have been reported in the literature regarding the wind-load effects on the structural deformation in HCPV solar trackers (Cancro et al., 2007; Gleckman, 2007; Luque-Heredia et al., 2006; Peterka et al., 1989). Although applications of the finite element analysis (FEA) technique in simulation of structural deformation for HCPV solar trackers have been conducted in a few studies (Cancro et al., 2007; Gleckman, 2007; Luque-Heredia et al., 2006), those studies did not consider the structural deformation of concentrator modules. Deformation of concentrator

modules could make the solar radiation deviate from the focal area on the cell. In this regard, deformation of concentrator modules and the associated tracking misalignment caused by gravity and wind loads should be included in the structural deformation analysis of an HCPV system. The aim of this study is, by means of finite element method, to develop a computer-aided engineering (CAE) analysis technique to assess the structural deformation and its induced solar tracking misalignment for design of a reliable HCPV solar tracking assembly. In particular, the effects of gravity and wind loads on the structural deformation in an HCPV system are characterized.

2. Modeling and validation

2.1. Modeling for structural deformation

A 3-D FEA model was constructed on the basis of a 5-kW HCPV system developed at Institute of Nuclear Energy Research (INER) using a commercial FEA code, ABAQUS. Structural deformation in the solar tracker at different zenith angles was calculated. Schematic of the FEA model at zenith angel of 63.5^{o} which is the maximum tracking angle of the solar tracker during operation is shown in Fig. 1. The system has a pedestal form of solar tracker attached with forty concentration modules. The dimension of one concentration module is 1338 × 555 × 246 mm^3 and the weight is about 19 kg. To simplify the model, fillets, chamfers, and drill holes in the components and gears of the driving mechanism were neglected. An 8-node hexahedral element was selected for most parts of the model. Hex-dominated elements (mixture of 8-node hexahedral and 4-node tetrahedral elements) were used for the remaining parts due to the sharp geometry. A complete FEA model was meshed with about 1,110,683 elements and 2,114,972 nodes.

Fig. 1: Schematic of finite element model for structural deformation simulation

2.2. Modeling for wind loads

The wind pressure distribution on the arrays of concentration modules at different wind speeds was determined using a commercial FEA code, COMSOL. The FEA model for wind loading calculation was constructed with three simplifications in order to reduce the computational time. Firstly, half of the HCPV structure and wind field were constructed due a symmetrical geometry. Secondly, only key components of the HCPV system were constructed, such as pedestal, concentration modules, rotating axle, and several steel beams. They are the major components facing the wind directly. Thirdly, the clearance between each concentration module in one array was neglected. Dimensions of the wind field are 30 × 40 × 60 m^3. Schematic of one half of the structure in the model is show in Fig. 2.

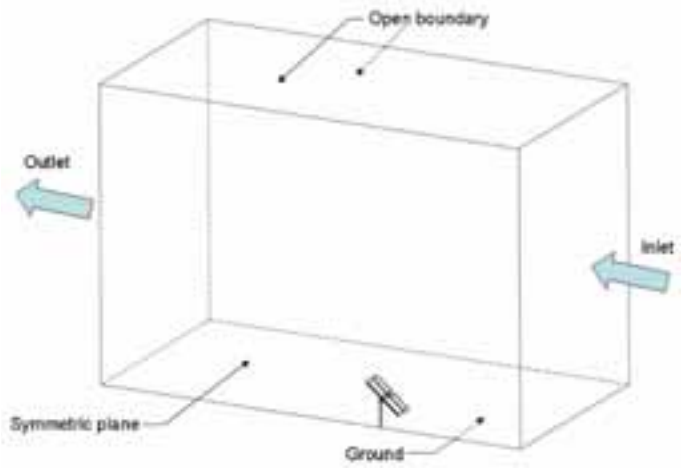

Fig. 2: Schematic of finite element model for wind load simulation

2.3. Investigated cases

In this study, three typical loading conditions were considered: gravity alone and wind blowing from front and back sides of the arrays of concentration modules. Eight zenith angles were considered in each loading condition, including 0^o, 10^o, 20^o, 30^o, 40^o, 50^o, 60^o, and 63.5^o. The wind blowing cases were carried out respectively for wind speeds of 7 and 12 m/s. These two wind speeds were chosen according to the operation guideline of the given HCPV system at INER.

2.4. Definition of Concentrator Misalignment

Concentrator misalignment is defined as the angle between the normal vector of the Fresnel lens and the direction of the solar beam. The method for calculating the concentrator misalignment due do structural deformation is described below. Four nodes at the corners and a node in the center of the Fresnel lens were selected. These five nodes construct four triangular planes. As shown in Fig. 3, each plane (*P*) has its original normal vector ($\vec{n}$) before deformation and has a new normal vector ($\vec{n}'$) after deformation. The angle α between vectors $\vec{n}$ and $\vec{n}'$ is the misalignment for the triangular lens plane. Consequently, four misalignment values were determined for one single Fresnel lens. In this study, the average of these four misalignment values was defined as the misalignment for each concentrator.

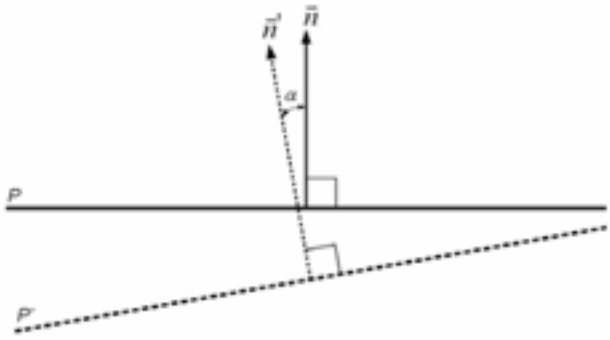

Fig. 3: Definition of the angle α between undeformed plane *P* and deformed plane *P'*

2.5. Deformation measurement and validation

In order to validate the constructed FEA model, simulation results were made a comparison with the measurements of strain change at two selected locations in the given HCPV system during field operation. Constantan alloy strain gauges with a length of 2 mm were used for measurements. Figure 4 shows the locations for strain measurement. Strain gauge *S1* was pasted on one of the four steel beams attached to the

twelve aluminum beams. Strain gauge *S2* was pasted on a steel ring extension which links the rotating axle and lead screws. A strainmeter was used to process the signals from the strain gauge. The strain data were then recorded and saved in a personal computer (PC). The experiment was performed in a sunny day without noticeable wind such that the experimental results were only made a comparison with the simulation for the case of gravity alone.

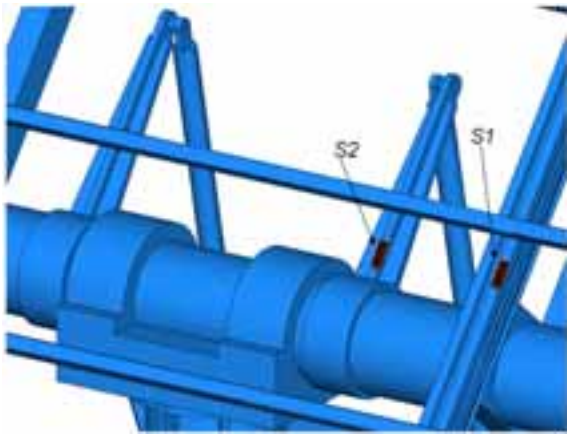

Fig. 4: Locations selected for strain measurement

3. Results and discussion

3.1. Effect of self-weight only

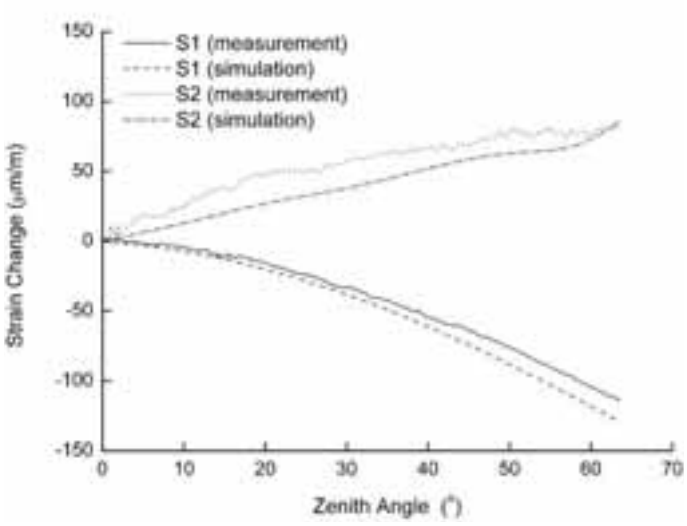

Fig. 5: Comparison of simulated and measured strain changes at various zenith angles

Figure 5 shows the simulated and measured strain changes as a function of zenith angle at two locations. By setting the strain value to zero initially at zenith angle of 0^o, the simulated strain change for each specified zenith angle was calculated by subtracting the calculated strain at zenith angle of 0^o from that at each specified zenith angle. As shown in Fig. 5, the strain measurements show that the strain change of gauge *S1* was decreased with an increase in zenith angle and the maximum strain change between 0^o and 63.5^o was 113 μm/m. The measured strain change of gauge *S2* was increased with zenith angle and the strain increment had a highest value of 80 μm/m at zenith angle of 63.5^o. The strain variation can be explained by the following structural analysis. At zenith angle of 0^o, the normal stress at location *S1* had a highest value because the steel beam was subjected to a maximum bending moment caused by the weight of concentration modules. The weight of concentration modules can be divided into two force components at zenith angle of

63.5°. One of the force components is normal to the steel beam and the other is parallel to it. The normal component of weight was less than that at zenith angle of 0° and it caused a smaller bending moment on the steel beam. Therefore, the stress and strain at location *S1* was decreased from zenith angle of 0° to 63.5°.

The steel ring extension attached with gauge *S2* was linked to the zenith rotating axle and it was subjected to a bending moment at location *S2* through the torque on the axle caused by the weight of concentration modules. At zenith angle of 0°, the weight of the upper and lower arrays of concentration modules was balanced about the zenith rotating axle and the torque on the axle was almost zero. The zenith rotating axle was subjected to a maximum torque at zenith angle of 63.5° leading to a maximum bending moment at location *S2*. Therefore, the stress and strain at location *S2* was increased with zenith angle. As shown in Fig. 5, the trend of strain change at each selected location in simulation agreed with that in measurement. The constructed FEA model for the given HCPV system was thus validated by such a reasonably good agreement.

Figure 6 shows the calculated distribution of von Mises equivalent stress in the steel beam at zenith angles of 0°. The maximum von Mises equivalent stress was of 76.2 MPa at zenith angles of 10° during rotation of the solar tracker from 0° to 63.5°. However, this value was very close to 75.4 MPa at zenith angles of 0°. The calculated maximum von Mises equivalent stress was less than the yield stress 250 MPa of an SS400 steel. Therefore, no structural failure (yielding/plastic deformation) was predicted for the given HCPV system at an operating condition without noticeable wind.

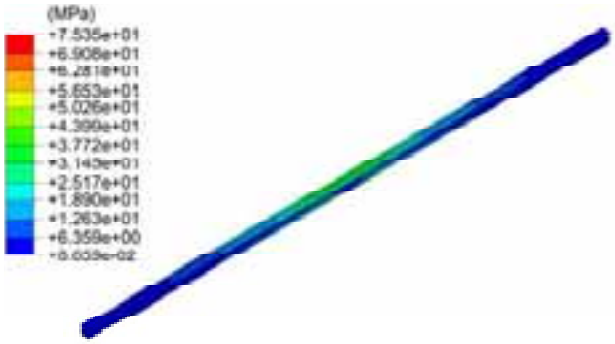

Fig. 6: Distribution of von Mises equivalent stress in the steel beam at zenith angles of 0° for gravity only (no wind)

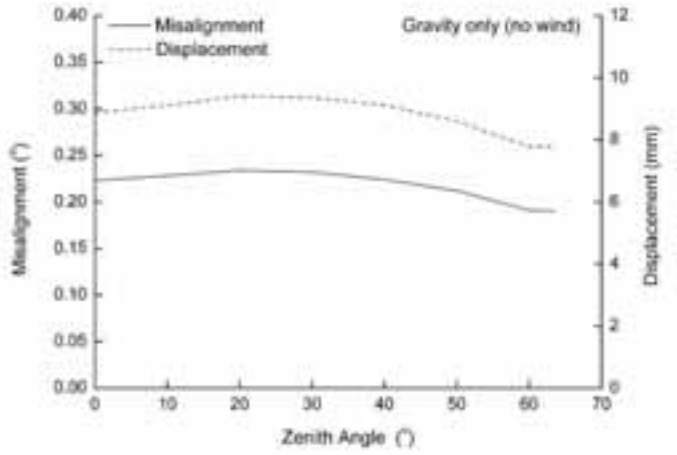

Fig. 7: Comparison of the maximum misalignment and displacement of concentrator modules at various zenith angles

Figure 7 shows the maximum misalignment and corresponding displacement of concentrators as a function of zenith angle. The resultant displacement of Fresnel lens in each concentrator includes contributions from the deformation of Fresnel lens and other components in the solar tracker. As shown in Fig. 7, the trend of variation in the maximum misalignment agreed with that of displacement. It means that the concentrators with greater misalignment could be readily identified from the corresponding displacement distribution. The

corresponding maximum displacement at zenith angles of 0°, 20°, 40°, and 63.5° were of 8.87, 9.4, 9.12, and 7.78 mm, respectively. The maximum concentrator misalignment for all the calculated conditions with gravity alone is 0.23° at zenith angle of 20°. This value is less than the acceptance angle of 0.4° for the given HCPV system. It indicates that gravity would not cause significant concentrator misalignment for the given HCPV system.

3.2. Effect of wind blowing to the front side of concentrator arrays

Figure 8 shows the calculated distribution of von Mises equivalent stress in the steel beam and steel ring extension at zenith angles of 0° and 63.5°, respectively, for a wind speed of 7 m/s blowing to the front side of the concentrator arrays. The locations where the maximum stress took place in these two components were the same as those in the case of gravity alone. The maximum von Mises equivalent stresses in the steel beam and steel ring extension during rotation of the solar tracker from zenith angle of 0° to 63.5° were of 76.1 MPa at 10° and 45.0 MPa at 63.5°, respectively. The corresponding values in the case of gravity alone were of 76.2 MPa at 10° and 38.6 MPa at 63.5°, respectively. Therefore, a wind speed of 7 m/s had no noticeable, additional effects on the stress distribution for the given solar tracker in comparison with the gravity effect alone. The stress distribution pattern in the case of a wind speed of 12 m/s blowing to the front side of the concentrator arrays was similar to that in Fig. 8. The maximum von Mises equivalent stresses in the steel beam and steel ring extension during rotation of the solar tracker from zenith angle of 0° to 63.5° were of 75.9 MPa at 10° and 62.6 MPa at 63.5°, respectively. It shows that a wind speed of 12 m/s had a greater effect on stress in the steel ring extension than did a wind speed of 7 m/s. However, 62.6 MPa was less than the yield stress 250 MPa of an SS400 steel.

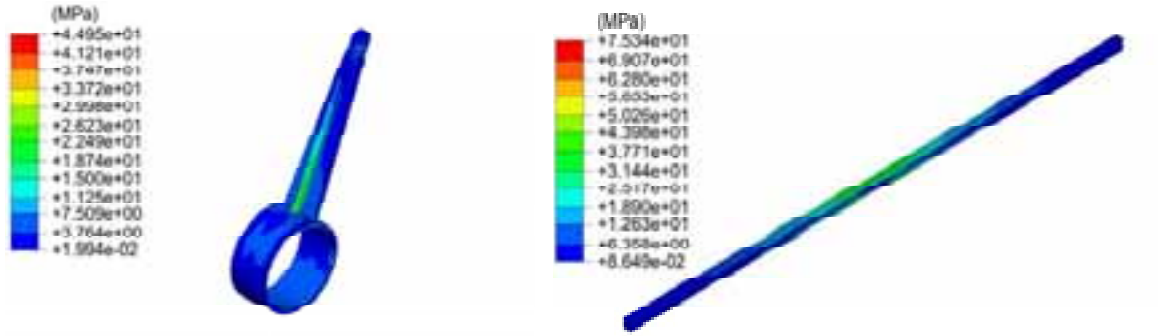

Fig. 8: Distribution of von Mises equivalent stress in the (a) steel beam at zenith angles of 0° and (b) steel ring extension at 63.5° for a wind speed of 7 m/s blowing to the front side of concentrator arrays

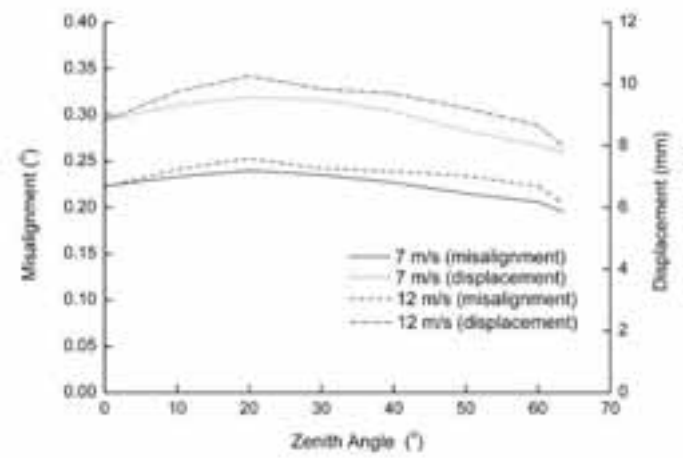

Fig. 9: Comparison of the maximum misalignment and displacement of Fresnel lens at various zenith angles for wind speeds of 7 and 12 m/s blowing to the front side of concentrator arrays

Figure 9 shows the maximum misalignment and corresponding displacement of concentrator modules as a

function of zenith angle for wind speeds of 7 m/s and 12 m/s blowing to the front side of concentrator arrays. The trend of variation in misalignment agreed with that of displacement, as shown in Fig. 9. As in the case of gravity alone (no wind), the concentrators with a greater misalignment value could also be readily identified from the corresponding displacement distribution in the wind blowing cases. The maximum displacement of Fresnel lens in the case of wind speeds of 7 and 12 m/s were of 9.65 mm at 30^o and 10.91 mm at 50^o, respectively. The maximum displacement of Fresnel lens in the case of a wind speed of 12 m/s are all greater than the corresponding ones in the case of gravity alone, indicating a wind speed of 12 m/s indeed generated an additional effect on the structural deformation and associated concentrator misalignment. The maximum concentrator misalignment for all the calculated conditions with a wind speed of 12 m/s blowing to the front side of concentration arrays is 0.3^o at zenith angle of 50^o. This value is less than the acceptance angle of 0.4^o.

3.3. Effect of wind blowing to the back side of concentrator arrays

For wind speeds of 7 and 12 m/s blowing to the back side of concentrator arrays, the patterns of stress distribution in the steel beam and steel ring extension were similar to those for wind blowing to the front side of concentrator arrays. The maximum von Mises equivalent stresses in the steel beam during rotation of the solar tracker form zenith angle of 0^o to 63.5^o for wind speeds of 7 and 12 m/s blowing to the back side of concentrator arrays were all equal to 75.4 MPa at 0^o and the maximum stresses in the steel ring extension were of 42.7 and 50.6 MPa at 63.5 ^{o} for 7 and 12 m/s, respectively. At zenith angle of 63.5^o, the maximum stresses in the steel beam and steel ring extension in the case of a wind speed of 7 m/s blowing to the back side of concentrator arrays were of 41.1 and 42.7 MPa, respectively. For a wind speed of 12 m/s, they were of 37.2 and 50.6 MPa, respectively. The corresponding values in the case of gravity alone were of 45.2 and 38.6 MPa, respectively. In comparison of these stress values, the stresses in the steel beam and steel ring extension were mainly contributed by the gravity for the case of a wind speed of 7 m/s blowing to the back side of concentrator arrays. Similar to the cases of wind blowing to the front side of concentrator arrays, the effect of wind blowing to the back side of concentrator arrays on the steel ring extension was greater than that on the steel beam. For all the calculated conditions with wind blowing to the back side of concentrator arrays, the maximum stress in the solar tracker during rotation of the solar tracker form zenith angles of 0^o to 63.5^o was less than the corresponding yield stress. Therefore, no plastic deformation was predicted to take place in the given solar tracker for a wind speed of 12 m/s and below.

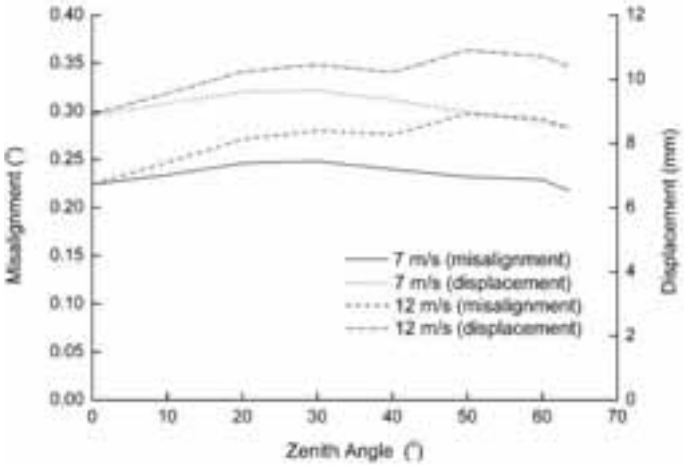

Fig. 10: Comparison of maximum misalignment and displacement of Fresnel lens at various zenith angles for wind speeds of 7 and 12 m/s blowing to the back side of concentrator arrays

Figure 10 shows the maximum misalignment and corresponding displacement of Fresnel lens in each concentrator as a function of zenith angle for wind speeds of 7 m/s and 12 m/s blowing to the back side of concentrator arrays. The trend of variation in misalignment agreed with that of displacement, as shown in Fig. 10. The concentrators with a greater misalignment value could also be identified from the corresponding displacement distribution in the wind blowing cases. For wind speeds of 7 and 12 m/s

blowing to the back side of concentrator arrays, the maximum concentrator misalignment was of 0.24° and 0.25° at zenith angle of 20°, respectively. In comparison of the two wind directions for a wind speed of 12 m/s, the maximum concentrator misalignment at each specified zenith angle for wind blowing to the back side of concentrator arrays was smaller than that for the other wind direction. It is because a greater deformation of the Fresnel lens in each concentrator was induced by the wind blowing toward the front side of concentrator arrays.

4. Conclusions

(1) An FEA model for the given HCPV system was constructed and validated to be effective in simulation of structural deformation and concentrator misalignment.

(2) During rotation of the given solar tracker, high stresses took place at two components, namely, the steel beam and steel ring extension. Based on the von Mises criterion, there was no stress value greater than the yield stress. Therefore, no structural failure (yielding/plastic deformation) was predicted for the given HCPV system at a normal operating condition.

(3) The trend of variation in the misalignment of a concentrator agreed with that in the resultant displacement of Fresnel lens of each concentrator so the concentrator with a greater misalignment could be readily identified from the corresponding displacement distribution.

(4) The maximum concentrator misalignment was of 0.23°, 0.25°, and 0.24° in the cases of no wind and a wind speed of 7 m/s blowing to the front side and back side of concentrator arrays, respectively. The maximum concentrator misalignment was of 0.3° and 0.25° in the cases of a wind speed of 12 m/s blowing to the front side and back side of concentrator arrays, respectively. These values were less than the acceptance angle of 0.4° for the concentrators in the given HCPV system. Therefore, the given HCPV system is expected to safely operate under a wind speed of 12 m/s and below with a high efficiency of solar power generation.

Acknowledgements

This work was supported by the National Science Council (Taiwan) under Contract No. NSC 98-2623-E-008-005-NU and by the Ministry of Economic Affairs (Taiwan) under Contract No. 98-EC-17-A-13-S2-0023.

References

Cancro, C., Graditi, G., Leanza, G., Pascarella, F., Sarno, A., Mancini, D., 2007. Field testing of the PhoCUS solar tracker by means of a novel optoelectronic device, in: Proceeding of the 4th International Conference on Solar Concentrators for the Generation of Electricity or Hydrogen.

Gleckman, P., 2007. A high concentration rooftop photovoltaic system, in: Proceeding of the SPIE (The International Society for Optical Engineering), Vol. 6649, pp. 664903-1-664903-10.

Luque, A., Hegedus, S., 2003. Handbook of Photovoltaic Science and Engineering, John Wiley & Sons, West Sussex, England.

Luque, A., Sala, G., Luque-Heredia, I., 2006. Photovoltaic concentration at onset of its commercial deployment. Prog. Photovolt.: Res. Appl. 14, 413-428.

Luque, A.L., Andreev, V.M., 2007. Concentrator Photovoltaics, Springer, Berlin.

Luque-Heredia, I., Quéméré, G., Magalhães, P.H., de Lerma, A.F., Hermanns, L., de Alarcón, E., Luque, A., 2006. Modelling structural flexure effects in CPV sun trackers, in: Proceeding of 21st European Photovoltaic Solar Energy Conference, pp. 2105-2109.

Peterka, J.A., Tan, Z., Cermak, J.E., Bienkiewicz, B., 1989. Mean and peak wind loads on heliostats. J. Sol. Energy Eng.-Trans. ASME 111, 158-164.

Willeke, G., 2003. High concentration photovoltaic–state-of-the-art and novel concepts, in: Proceeding of the 3rd World Conference on Photovoltaic Energy Conversion, pp. 2841-2844.